6334 J. Phys. Chem. A 2009, 113, 6334–6341

Influence of Resonance Interactions and Matrix Environment on the Spectra of SF_6 Dimers in Low-Temperature Nitrogen Matrixes. Theory and Experiment

Irina K. Tokhadze, Tatjana D. Kolomiitsova, Dmitrii N. Shchepkin, and Konstantin G. Tokhadze*

Physical Faculty, St. Petersburg State University, Peterhof, St. Petersburg 198504, Russia

Zofia Mielke

Faculty of Chemistry, University of Wrocław, Joliot Curie 14, Wrocław50-383, Poland

Received: March 6, 2009; Revised Manuscript Received: April 17, 2009

The IR absorption spectra of $(SF_6)_2$ dimers were studied in N_2 matrixes at 11 K. Absorption bands due to SF_6 monomers and to $(SF_6)_2$ dimers have been identified. As a result of the resonance dipole−dipole interaction between two SF_6 subunits, the band of the triply degenerate vibration ν_3 is split into two components $\nu_{X},_{Y}$ and ν_Z, where Z is the axis connecting the two sulfur atoms. The main distinction between the spectra of $(SF_6)_2$ dimers recorded here compared to spectra in the gas phase is the splitting of the $\nu_{X},_{Y}$ component. A model that takes into account the influence of the matrix on the spectra of dimers is developed. The model makes it possible to successively (i) calculate the resonance spectrum of an isolated dimer in terms of the model of local modes including the resonance interactions, (ii) determine with the help of the Monte Carlo method the structure of a matrix consisting of 864 N_2 molecules and a rigid $(SF_6)_2$ dimer, and (iii) take into account the interactions of local dipole moments of a dimer with host particles in the approximation of dipole−induced dipole and dipole−quadrupole interactions. The calculated spectra sufficiently well reproduce the main characteristics of the experimental spectra in N_2 matrixes, in particular, the decrease of the resonance splitting upon transition from the gas phase to a matrix and the splitting of $\nu_{X,Y}$ component in the nitrogen matrix.

I. Introduction

The IR spectra of van der Waals dimers, consisting of molecules of O_h or T_d symmetry, have been extensively studied during the last 30 years.[1−10] The binding energy of such complexes is small ($\Delta E < 100-200$ cm^{-1}); therefore, their spectra were recorded at low temperatures, $T < 90$ K, using various experimental techniques. For the example of the $(SF_6)_2$,[1−3,11−15] $(SiF_4)_2$,[1,6,8,16] and $(SiH_4)_2$[3] dimers, it has been shown that the resonance dipole−dipole (RDD) interaction between two partner molecules plays a decisive role in the formation of the absorption spectra of these complexes.[4,7] Because the $(SF_6)_2$ dimer has no dipole moment, it is not observable by microwave spectroscopy, the widely used method for studying van der Waals dimers.

The characteristic feature of these spectra in the region of the fundamental absorption is the splitting of the three-fold degenerate ν_3 vibration due to the RDD interaction. It has been shown[4,15] that the magnitude of this splitting is proportional to the square of the dipole moment derivative P'_3 with respect to the dimensionless normal coordinate, $\Delta\nu = 3\boldsymbol{a}$, where $\boldsymbol{a} = (P'_3)^2/(2hcR^3)$ and R is the distance between the centers of gravity of the subunits. A small contribution to the splitting of the ν_3 band of a dimer is made by the interaction of the dipole−induced-dipole (DID) type, $\Delta\nu = 3\boldsymbol{a}(1+\beta)$, where $\beta = \alpha/R^3$ and α is the polarizability of the partners.

The degenerate ν_3 fundamental transition in SF_6 is one of the strongest transitions in IR spectroscopy,[17] and the resonance splitting value that is proportional to the band intensity is about 20 cm^{-1} for this transition. This has been the reason for permanent interest of both experimentalists and theoreticians in IR spectra of SF_6 clusters. However, we are aware of only a single experiment devoted to the study of the vibration−rotation spectra of $(SF_6)_2$ dimers in the molecular beam at $T_{rot} \approx 1$ K.[13] Under these conditions, two absorption bands are observed for $(SF_6)_2$; one band (ν_Z) is 14 cm^{-1} red shifted and the other ($\nu_{X,Y}$) is 8 cm^{-1} blue shifted from the ν_3 band. The ν_Z band is the parallel band with the resolved rotational structure, and the $\nu_{X,Y}$ band is the doubly degenerate perpendicular band. The measured parameters of these vibration−rotation bands make it possible to determine the structural and geometric characteristics of $(SF_6)_2$ dimers. The $(SF_6)_2$ dimer was found to have D_{2d} symmetry, with the distance between the S atoms of $R_{ss} = 4.754$ Å, and the resonance splitting of $\Delta\nu = \nu_{X,Y} - \nu_Z = 22.1$ cm^{-1}.

The first studies of $(SF_6)_2$ and $(SiF_4)_2$ dimers in low-temperature matrixes[15,16,18] demonstrated the efficiency of this technique in studying the resonance interactions and the influence of a medium on spectral characteristics of van der Waals complexes. On the whole, the absorption spectra of these dimers in matrixes proved to be similar to the spectra of dimers in molecular beams[11,12] and in solutions in liquefied noble gases,[7,19] although, in the latter case, noticeably broader absorption bands were observed. In low-temperature matrixes, it is possible to observe the vibrational band structure of dimers and to measure accurately the splitting values. These data can form the basis for the development of more complicated models, which, in particular, will be capable of describing the effect of a matrix on the spectral characteristics. In this case, it is necessary to recognize that changes in the spectra of dimers in inert matrixes can be connected not only with the effect of the

---

* To whom correspondence should be addressed. E-mail: K.Tokhadze@molsp.phys.spbu.ru.

10.1021/jp902055m CCC: $40.75

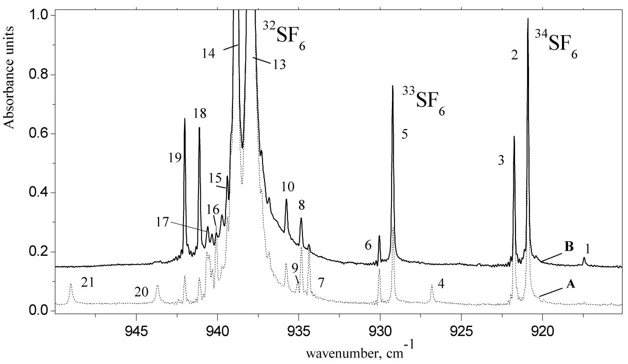

Figure 1. The ν_3 region in the spectra of the SF_6/N_2 =1/2000 matrix with the natural abundance of sulfur isotope. Spectra were recorded at 11 K after deposition (A) at 17 K and after annealing (B) at 30 K. The bands labeled by $^{32}SF_6$, $^{33}SF_6$, and $^{34}SF_6$ are the ν_3 monomer bands of isotopomers. The components of these bands are marked by 1, 2,..., 21.

environment on the spectral parameters of the system but also with changes in the structural characteristics of dimers.

In this paper, we present the results of FTIR and molecular simulation studies of the $(SF_6)_2$ dimer spectra in nitrogen matrixes. The spectra of $(SF_6)_2$ in N_2 matrixes in the ν_3 spectral region are compared with the spectra of $(SF_6)_2$ in Ar matrixes under the same conditions.[15] By using the computer simulation method, we attempted to determine the effect of a matrix on the spectra of the $(SF_6)_2$ dimers. The method developed involves the calculation of the resonance spectrum of an isolated dimer with the help of the local-mode model, the simulation by the Monte Carlo method of the structure of the N_2 matrix containing the rigid (SF_6) dimer, and the calculation of the interaction of the local dipoles of the dimer with the particles of the matrix.

II. Experimental Section

Gas mixtures of the SF_6 and N_2 were prepared by the standard manometric technique. The concentration of SF_6/N_2 mixtures was varied in the range of 1/500−1/6000. The gas mixtures were sprayed onto a gold-plated cold mirror held at 19 K during matrix deposition by means of a closed cycle helium refrigerator (Air Product Displex 202A), and the matrix was maintained at 11 K for the infrared measurements.[20] Spectra were recorded at 0.1 cm^{-1} resolution in reflection mode with a Bruker 113v FTIR spectrometer.

Nitrogen with a purity of 99.99% was obtained from POLGAS, Poland; SF_6 with the natural abundance of sulfur isotopes (^{32}S, 95.06%; ^{33}S, 0.74%; ^{34}S, 4.18%; ^{36}S, 0.016%) was obtained from Institute of Applied Chemistry, Russia.

III. Results

The infrared spectra of SF_6 dimers were studied in nitrogen matrixes. The spectra were recorded in the ν_3 region of SF_6 with the matrix concentration increasing from SF_6/N_2 = 1/6000 to 1/500. Figure 1 shows the ν_3 region in the spectra of the SF_6/N_2 = 1/2000 matrix with the natural abundance of sulfur isotopes. The spectra were recorded at 11 K after matrix deposition at 17 K (curve A) and after annealing at 30 K (curve B). One can see in Figure 1 that some additional bands were observed on the high-frequency and low-frequency wings of the ν_3 monomer band of the $^{32}SF_6$ molecule. For each isotopomer, the ν_3 monomer band has a characteristic site structure that includes two components indicated by numbers 2 and 3 for $^{34}SF_6$, 5 and 6 for $^{33}SF_6$, and 13 and 14 for $^{32}SF_6$, respectively.

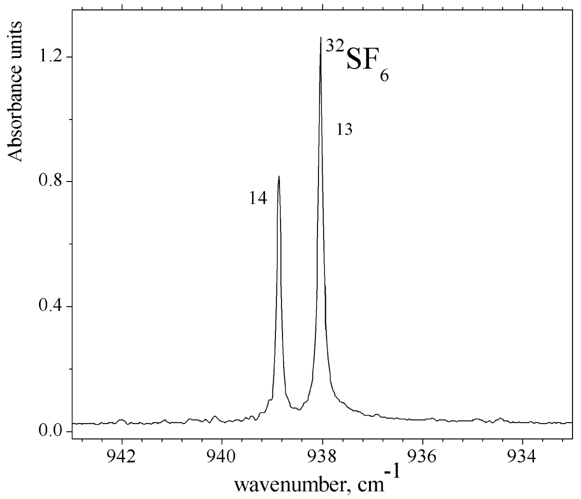

Figure 2. The ν_3 monomer band of the $^{32}SF_6$ molecule in the spectra of the SF_6/N_2 = 1/6000 matrix recorded at 11 K after deposition at 17 K.

The ν_3 monomer band of $^{32}SF_6$ in the spectra of the SF_6/N_2 = 1/6000 is presented in Figure 2.

We calculated the relative intensities $I_{rel} = B_n/B_{34}$ for all of the bands in the spectra of SF_6/N_2, where B_n is the integrated intensity of the band labeled by number n and $B_{34} = B_2 + B_3$ is the integrated intensity of two site components 2 and 3 of the ν_3 band of a $^{34}SF_6$ monomer. The spectra in the ν_3 region of $^{34}SF_6$ are insensitive to the dimer concentration if $SF_6/N_2 <$ 1/500 and the B_{34} value is proportional to the monomer concentration with good accuracy. The concentration dependences of the relative intensity of all bands were studied after deposition and after annealing. The recorded bands were assigned to monomers or to dimers of SF_6 molecules on the basis of comparison of concentration dependences. The relative intensities of monomer bands are independent of the matrix concentration, while the dimer band intensities linearly increase ($I_{rel}(\text{dimer}) = \zeta \cdot C + b$) with the matrix concentration C. The concentration dependences of some monomer and dimer bands are presented in Figure 3. The frequencies, full widths at half-maximum (fwhm), and relative intensities of these bands in the spectra of SF_6/N_2 = 1/2000 matrixes at 11 K are listed in Table 1.

The dimer bands can be divided into two groups. The intensity of the bands belonging to the first group increases with matrix concentration both after deposition and after matrix annealing. The intensities of these bands increase significantly after matrix annealing. Three strong bands at 929.2, 941.1, and 942.0 cm^{-1} indicated in boldface in Table 1 by numbers 5, 18, and 19, respectively, and three weak bands at 917.4, 935.8, and 943.7 indicated by numbers 1, 10, and 20, respectively, belong to this group. The dimer band at 929.2 cm^{-1} coincides with the low-frequency site of the $^{33}SF_6$ monomer band. The band at 943.7 cm^{-1} splits into three components at 943.5, 943.7, and 943.9 cm^{-1} after annealing.

Three weak bands at 926.8, 940, and 949.0 cm^{-1} indicated by numbers 4, 16, and 21, respectively, belong to the second group. Their intensities after deposition increase with matrix concentration, but these bands disappear after annealing.

IV. Discussion

Following the previous studies,[9,13,14] we have described the spectra of SF_6 dimers in the fundamental ν_3 region using first a simple model in which the splitting of the triply degenerate ν_3

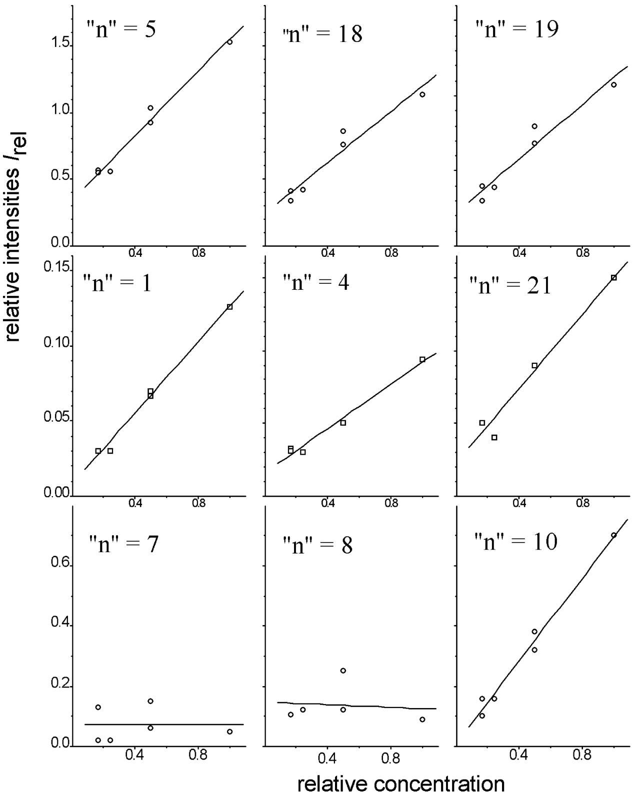

Figure 3. Concentration dependences of the relative intensities $I_{\mathrm{rel}} = \xi \cdot C + b$ of absorption bands are marked by $n = 1, 2,...$ in the spectra of SF$_6$/N$_2$ matrix. "n": **5**: $\nu = 929.3$ cm^{-1}, $\xi = 1.2(1)$, $b = 0.3(1)$; **18**: 941.1 cm^{-1}, $\xi = 1.0(1)$, $b = 0.2(1)$; **19**: 942.0 cm^{-1}, $\xi = 0.9(1)$, $b = 0.2(1)$; **1**: 917.4 cm^{-1}, $\xi = 1.2(1)$, $b = 0.02(1)$; **4**: 926.8 cm^{-1}, $\xi = 0.15(1)$, $b = 0.03(1)$; **21**: 949.0 cm^{-1}, $\xi = 0.25(5)$, $b = 0.03(1)$; **7**: 934.4 cm^{-1}, $\xi = 0.0(1)$, $b = 0.08(10)$; **8**: 934.8 cm^{-1}, $\xi = 0.0(1)$, $b = 0.15(10)$; **10**: 935.8 cm^{-1}, $\xi = 0.70(5)$, $b = 0.0(1)$.

mode is governed primarily by the resonance dipole−dipole (RDD) interaction between two molecules. In this model, it is assumed that the dimer consists of two structureless, triply degenerate oscillators labeled as 1 and 2 with the Cartesian normal coordinates X_i, Y_i, Z_i ($i = 1, 2$), and the Z axis is directed along the dimer axis.

If we take into account the additional contribution of the dipole−induced-dipole (DID) interaction between the SF$_6$ molecules, the splitting $\Delta\nu$ in the dimer is given by

$$\Delta\nu = \nu_{X,Y} - \nu_Z = 3\boldsymbol{a}(1 + \beta) \tag{1}$$

where $\boldsymbol{a} = (P'_3)^2/(2hcR_{\mathrm{SS}}^3)$, P'_3 is the dipole moment derivative of the monomer SF$_6$ with respect to the dimensionless normal coordinate Q$_3$, R_{SS} is the S−S distance, $\beta = \alpha/R_{\mathrm{SS}}^3$ is a dimensionless parameter, and α is the isotropic polarizability of SF$_6$. The ratio of the intensity of the lower-frequency component (I_Z), red shifted from the ν_3 band, to the intensity of the higher-frequency component ($I_{X,Y}$), blue shifted from the ν_3 band, is described by the expression

$$\zeta = \frac{I_Z}{I_{X,Y}} = \frac{(1 + \beta)^2}{2(1 - 2\beta)^2} \tag{2}$$

The polarizability of SF$_6$ is 6.558 Å^3,[22] the intermolecular separation obtained from vibration−rotation spectra of (^{32}SF$_6$)$_2$ in a molecular beam is $R_{\mathrm{SS}} = 4.754$ Å^3,[13] and $P'_3 = 0.551$ D,[17] which leads to $\boldsymbol{a} = 5.86$ cm^{-1}, $\beta = 0.061$, and $\zeta = 0.73$.

This simple model with the resonance dipole−dipole interaction between point dipole moments located at the centers of mass of each SF$_6$ molecule predicts the main spectral features of (SF$_6$)$_2$ dimers in the gas phase and in argon matrixes. However, even for the gas phase, the calculation does not predict the resonance splitting in good agreement with the experimental value, namely, the calculated result $\Delta\nu_{\mathrm{calc}} = 18.65$ cm^{-1} is smaller than the experimental value of $\Delta\nu = 22.1$ cm^{-1}.

The doublet 4, 21 can be assigned to the dimer whose parameters are similar to parameters of the (^{32}SF$_6$)$_2$ dimer in the gas phase, namely, the relative intensity $\zeta = (I_Z^*)/(I_{X,Y}^*) = (I_4)/(I_{21}) = 0.56$, and the splitting value is equal to $\Delta\nu = \nu_{X,Y}^* - \nu_Z^* = \nu_{21} - \nu_4 = 949.0 - 926.8 = 22.2$ cm^{-1}. Note once again that this dimer exists only after deposition and disappears after matrix annealing.

The spectrum of the (SF$_6$)$_2$ dimer in the nitrogen matrix strongly differs from the dimers' spectra in the argon matrix[15] and those in the gas phase.[13] In solid nitrogen, the (^{32}SF$_6$)$_2$ dimer is characterized by a triplet with ν_X (ν_{18}) $= 941.1$ cm^{-1}, ν_Y (ν_{19}) $= 942.0$ cm^{-1}, and ν_Z (ν_5) $= 929.2$ cm^{-1}; the intensity ratio is $I_X \approx I_Y \approx 0.78 \times I_Z$. The X and Y components of the resonance doublet are split in this matrix by $\delta = |\nu_Y - \nu_X| = 0.9$ cm^{-1}. The value of resonance splitting $\Delta\nu = (\nu_X + \nu_Y)/2 - \nu_Z$ is equal to ~12.4 cm^{-1}. The spectra of all of the isotopomers of SF$_6$ in the N$_2$ matrix are identical (Table 2).

The weak band 1 is due to the mixed (^{32}SF$_6$−^{34}SF$_6$) dimer. In the spectra of SF$_6$ with the natural isotope abundance, the relative concentrations of the dimers are 0.904 for (^{32}SF$_6$)$_2$, 0.002 for (^{34}SF$_6$)$_2$, 0.014 for (^{32}SF$_6$−^{33}SF$_6$), and 0.079 for (^{32}SF$_6$−^{34}SF$_6$). The use of the approach described in ref 15 allowed us to calculate the mixed ^{32}SF$_6$−^{34}SF$_6$ dimer spectrum, which is characterized by four bands whose frequencies and relative intensities (in parentheses) are equal $\nu(Z^-) = 917.4$ (0.073), $\nu(Z^+) = 941.7$ (0.012), $\nu(X(Y)^-) = 919.7$ (0.037), and $\nu(X(Y)^+) = 938.6$ cm^{-1} (0.097). To calculate the spectral parameters of the mixed dimers in nitrogen matrixes, we used the effective resonance parameter $\boldsymbol{a}_{\mathrm{eff}} = (\boldsymbol{a} \cdot \boldsymbol{a}^*)^{1/2} = 3.85$ cm^{-1}, where $\boldsymbol{a}$ and $\boldsymbol{a}^*$ are the resonance parameters of unlike isotopomers. The stronger band of this quadruplet at 938.6 cm^{-1} coincides with the low-frequency site of the ^{32}SF$_6$ monomer band.

V. Model Calculation of an Isolated (SF$_6$)$_2$ Dimer Spectrum

Influence of matrix environment on the spectral characteristics of (SF$_6$)$_2$ dimers can be analyzed with the help of a model that allows us to successively describe the absorption spectrum of a free SF$_6$ molecule and, then, the spectrum of (SF$_6$)$_2$ dimer, which is mainly formed by the resonance dipole−dipole interactions, and to calculate the spectral effects of the interaction between the dimer and matrix particles. The structure of matrixes doped with (SF$_6$)$_2$ dimers can be determined using the computer simulation methods.

To describe the SF$_6$ dimer spectra in the ν_3 region, we use the local-mode model[18,21,23] in which the SF$_6$ molecule is characterized by six point dipole moments located on each of the S−F bonds. Each dipole moment is shifted along the S−F bond by f (Å) relative the center of the SF$_6$ molecule, $0 < f < R_{\mathrm{SF}}$, where R_{SF} is the SF bond length (see Figure 4). The spectra of the (SF$_6$)$_2$ dimer are formed by the resonance dipole−dipole interactions between the point dipole moments of two molecules 1 and 2 separated by a distance R_{SS}. Under these assumptions,

TABLE 1: Experimental Frequencies ν (cm^{-1}), FWHM (cm^{-1}), and Relative Intensities I_{rel} of the Bands in the ν_3 Region in the Spectra of SF_6/N_2 = 1/2000 Matrixes at 11 K

≪*n*≫	assignment	ν	fwhm	I_{rel} after deposition	I_{rel} after annealing
1	$^{32}S-^{34}S$, d(*Z*)	917.4	0.15	0.03	0.07
2	^{34}S, m	920.9	0.12	0.62	0.67
3	^{34}S, m	921.75	0.10	0.38	0.33
4	^{32}S, d(*Z*)	926.8	0.15	0.10	0.0
5	**^{33}S, m + ^{32}S, d(*Z*)**	**929.2**	**0.12**	**0.47**	**1.09**
6	^{33}S, m	930.05	0.10	0.06	0.05
7	^{32}S, m	934.4	0.12	0.25	0.15
8	^{32}S, m	934.8	0.13	0.25	0.25
9	^{32}S,	935.1	0.15	~0.10	0.0
10	^{32}S, d	935.8	0.20	0.20	0.40
11	^{32}S, m	936.8	0.2	~0.10	~0.10
12	^{32}S, m	937.3	0.3	~0.15	~0.15
13	^{32}S, m	938.05	0.10	14.1[a]	15.2[a]
14	^{32}S, m	938.85	0.10	8.6[a]	7.5[a]
15	^{32}S, m	939.5	0.3	0.6	0.6
16	^{32}S, d	940.1	0.15	~0.5	~0.1
17	^{32}S, m	940.5	0.20	~0.4	0.0
18	**^{32}S, d(*X*)**	**941.1**	**0.14**	**0.32**	**0.85**
19	**^{32}S, d(*Y*)**	**942.0**	**0.11**	**0.28**	**0.80**
20	^{32}S, d	943.7	0.30	0.18	~0.1
21	^{32}S, d(*X*,*Y*)	949.0	0.25	0.18	0.0

[a] These intensities were calculated using the experimental values of the relative intensities I_1 and I_2 for the two site components of the ν_3 monomer band of $^{34}SF_6$ and the natural abundance of the sulfur isotope. [b] The lines indicated in boldface correspond the most stable dimer bands.

TABLE 2: Observed Frequencies ν (cm^{-1}) and Splitting Values $\Delta\nu = \nu_{X,Y} - \nu_Z$, $\delta = |\nu_Y - \nu_X|$, and $\nu_{X,Y} = (\nu_X + \nu_Y)/2$ (cm^{-1}) for SF_6 Dimers of Like Isotopomers in Solid Nitrogen at 11 K[a]

parameter	$^{32}SF_6-^{32}SF_6$	$^{33}SF_6-^{33}SF_6$	$^{34}SF_6-^{34}SF_6$
ν_X	941.1(1)	932.2(1)	923.4(1)
ν_Y	942.2(1)	933.0(1)	924.7(1)
ν_Z	929.2(1)	920.4(1)	912
$\Delta\nu$	12.4(5)	12.2(3)	12.1(2)
δ	0.9	0.8	1.3

[a] The $(^{33}SF_6)_2$ and $(^{34}SF_6)$ dimer bands were observed in the spectra of SF_6/N_2 > 1/800 matrixes.

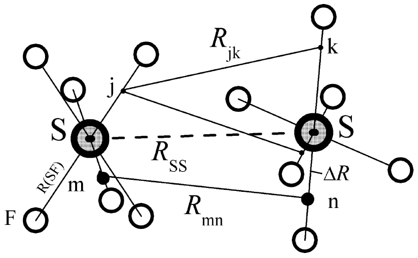

Figure 4. Schematic of interactions in the $(SF_6)_2$ dimer in the local-mode approximation; Δ*R* is the distance of a point local dipole from the center of the S atom and R_{jk} and R_{mn} are the distances between dipoles on different bonds. The dimer has D_{2d} symmetry.

the dimer spectrum should strongly depend on relative orientation of molecules in the $(SF_6)_2$ dimer. Analysis of the spectra can provide information on the changes in the dimer structure.

The dipole moment $\vec{P}$ of a dimer is a vector sum of the dipole moments of individual molecules $\vec{P} = \vec{P}_1 + \vec{P}_2$. The dipole moments of the molecules are $\vec{P}_1 = \sum_i P_i \vec{e}_i$ and $\vec{P}_2 = \sum_k P_k \vec{e}_k$, where P_i and P_k are the norms of the dipole moments that can be written for a bond *j* as $P_j = P_{j0} + \partial P_j/\partial q_j \cdot \partial q_j$, where $\partial P_j/\partial q_j$ is the derivative of the dipole moment of the bond with respect to its change, which can be calculated from the dipole moment derivative P'_3 with respect to the dimensionless normal coordinate. For the SF_6 molecule (O_h symmetry) $\partial P_j/\partial q_j = 1/(2)^{1/2} \cdot P'_3$.

The spectrum of noninteracting SF_6 molecules is used as a zero-order approximation. To describe the stretching vibrations of noninteracting molecules, it is expedient to apply the model of local modes.[21] In this model, each of the SF_6 molecules is modeled by six harmonically coupled Morse oscillators, and the zero-order Hamiltonian is represented in the form

$$H^0 = \sum_{j=1}^{6}\left[D(1 - \exp(-\eta r_j)^2) + \frac{p_j^2}{2\mu}\right] \tag{3}$$

where *j* labels the bonds, η and *D* are the Morse potential parameters, μ is the SF reduced mass, r_j is an internal coordinate, and p_j is the conjugate momentum. As a perturbation $\hat{V}$, the harmonic coupling of oscillators is considered

$$\hat{V} = \frac{1}{m}\sum_{j,k}^{6}(\cos\theta_{jk} p_j p_k + f^*(r_j r_k + ...)) \tag{4}$$

where *m* is the mass of the central S atom, $\theta_{jk}$is the angle between the bonds, and f^* is the coupling force constant. The zero-order basis set consists of products of six eigenfunctions of Morse oscillators with vibrational quantum number V_j

$$\prod_{j=1}^{6}\psi_{V_j}(r_j) \equiv \langle V_1V_2V_3V_4V_5V_6|$$

The corresponding eigenvalues are given by

$$E_{V_j} = \sum_{j=1}^{6}\left(\omega\left(V_j + \frac{1}{2}\right) - x\cdot\left(V_j + \frac{1}{2}\right)^2\right) \tag{5}$$

where $\omega = (2\eta^2 D/\mu)^{1/2}$ is the harmonic frequency of the diatomic SF molecule, $x = -\omega\eta^2/2\gamma$ is the Morse anharmonicity parameter, and $\gamma = 4\pi^2 c\omega\mu/h$. For the SF_6 molecule,[21] $x = 3.5$ cm^{-1}, $\omega = 880$ cm^{-1}, $\mu = 11.92$ amu, and $(\gamma)^{1/2} = 17.6$ Å^{-1}. Taking into account the kinematic and dynamic interactions of individual oscillators, we obtain the 6 × 6 matrix [*b*], whose eigenvalues $\nu_3 = 948$, $\nu_1 = 776$, and $\nu_2 = 644$ cm^{-1} are close to the frequencies of the stretching vibrations of a free SF_6 molecule, $\nu_3 = 948$, $\nu_1 = 774$, and $\nu_2 = 643.4$ cm^{-1}.[21]

We will take into account only the resonance dipole−dipole (RDD) interactions between individual oscillators of the two molecules forming a $(SF_6)_2$ dimer. The frequencies, intensities, and expansion coefficients of the normal modes of the $(SF_6)_2$ dimer in internal coordinates can be obtained by solving the secular equation of the 12th order

$$\begin{vmatrix} [b] & W_{12} \\ W_{21} & [b] \end{vmatrix} = 0 \tag{6}$$

where submatrixes W_{21} and W_{12} in secular eq 6 describe the RDD interaction of two identical molecules 1 and 2. The matrix element that describes interaction between the *j*th bond of molecule 1 and the *k*th bond of molecule 2 can be written as

$$\begin{aligned} W_{jk} &= \frac{\left(\frac{\partial P_j}{\partial q_j}\right)\left(\frac{\partial P_k}{\partial q_k}\right)}{2hc}\left[\frac{(\vec{e}_j\vec{e}_k)}{R_{jk}^3} - 3\frac{(\vec{e}_j\vec{e}_{jk})(\vec{e}_k\vec{e}_{jk})}{R_{jk}^3}\right] \\ &= \frac{(P'_3)^2}{4hc}\left[\frac{(\vec{e}_j\vec{e}_k)}{R_{jk}^3} - 3\frac{(\vec{e}_j\vec{e}_{jk})(\vec{e}_k\vec{e}_{jk})}{R_{jk}^3}\right] \end{aligned} \tag{7}$$

where $\vec{R}_{jk} = R_{jk}\vec{e}_{jk}$is the radius vector that connects the point dipoles of the interacting bonds (Figure 4). The unit vectors $\vec{e}_j$ and $\vec{e}_{jk}$ specify the orientation of the *j*th SF bond and R_{jk} vector. The radius vector $\vec{R}_{jk}$ depends on the geometric configuration of the dimer and on the model parameter $\boldsymbol{f} = \Delta R/R(SF)$ that determines the position of point dipole moment relative to the central atom, where ΔR is the distance of a point-like local dipole from the center of the S atom and R(SF) is the length of the SF bond.

The solution of the secular eq 6 gives the frequencies and intensities of the 12 stretching vibrations of $(SF_6)_2$ dimers. To compare the theoretical and experimental results, it is necessary to additionally take into account the changes in the dimer frequencies due to DID interactions between SF_6 molecules.[15] In this approximation

$$\nu_Z^* = \nu_Z^{\mathrm{LM}} - 4\boldsymbol{a}\beta \qquad \nu_{X,Y}^* = \nu_{X,Y}^{\mathrm{LM}} - \boldsymbol{a}\beta \tag{8}$$

and $\Delta\nu = 3\boldsymbol{a}(1 + \beta)$, where ν_Z^{LM} and $\nu_{X,Y}^{\mathrm{LM}}$ are the calculated frequencies. For $(SF_6)_2$, the correction parameter is $3\boldsymbol{a}\beta = 1.3$ cm^{-1}. At $\boldsymbol{f} = 0.7$, the calculated splitting value is 955.3 − 934.7 = 20.6 cm^{-1}. Upon taking into account the DID interaction, this value increases up to $\Delta\nu = 20.6 + 1.3 = 21.9$ cm^{-1}, which proves to be close to the experimental value $\Delta\nu = 22.07$ cm^{-1} for $(SF_6)_2$ in the gas phase.[13]

VI. The Interaction of the $(SF_6)_2$ Dimers with the Host Particles

Using the local-mode model allows us to analyze the influence of the matrix environment on the dimer spectra. In the nitrogen matrix, the DID interaction between the dipole under study and the host particles will be considered as a perturbation. The field of the *j*th dipole of the $(SF_6)_2$ dimer induces a dipole on the *m*th particle (Figure 5), and the energy of an interaction of an induced dipole with the *k*th dipole of the dimer ($j = 1,..., 12$; $k = 1,..., 12$) is

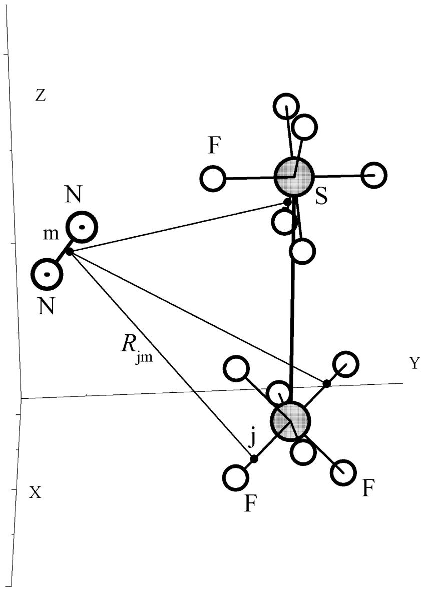

Figure 5. Schematic of interactions of the $(SF_6)_2$ dimer with nitrogen molecules in a matrix in the local-mode approximation; R_{jm} is the distance between a local dipole on one of the bonds of the dimer and the center of the N_2 molecule.

$$\begin{aligned} \Delta U_{jkm} &= \frac{1}{2}\left(\frac{(\vec{\mathrm{P}}_{jm}^{(\mathrm{ind})}, \vec{P}_k)}{(\vec{R}_{km})^3} - 3\frac{(\vec{\mathrm{P}}_{jm}^{(\mathrm{ind})}, \vec{R}_{km})(\vec{P}_k, \vec{R}_{km})}{(\vec{R}_{km})^5}\right) \\ &= \frac{1}{2}\left(P_j^0 + \left(\frac{\partial P_j}{\partial q_j}\right)q_j\right)\cdot\left(P_k^0 + \left(\frac{\partial P_k}{\partial q'_k}\right)q_k\right)\cdot\Theta_{jkm} \end{aligned} \tag{9}$$

where

$$\Theta_{jkm} = \frac{(\hat{\alpha}\vec{s}_{jk}, \vec{e}_k)}{(\vec{R}_{km})^3} - 3\frac{(\hat{\alpha}\vec{s}_{jm}, \vec{R}_{km})(\vec{e}_k, \vec{R}_{km})}{(\vec{R}_{km})^5} \qquad \vec{s}_{jm} = 3(\vec{e}_j\cdot\vec{R}_{jm}) \times \frac{\vec{R}_{jm}}{(\vec{R}_{jm})^5} - \frac{\vec{e}_j}{(\vec{R}_{jm})^3}$$

Here, $\hat{\alpha}$ is the polarizability tensor of the *m*th particle of a matrix (for an argon atom, the polarizabilaty is scalar), $j = 1-6$ for the first SF_6 molecule, $j = 7-12$ for the second SF_6 molecule, and $\vec{R}_{jm}$ is the distance between the *j*th dipole moment of the $(SF_6)_2$ and the *m*th particle.

The elements of the 12 × 12 matrix in eq 6, which describe the dimer absorption spectrum, should be supplemented with diagonal ($\Delta W_{1,1}$, $\Delta W_{2,2}$, $\Delta W_{12,12}$,...) and off-diagonal ($\Delta W_{1,2}$,$\Delta W_{1,3}$,..., $\Delta W_{1,12}$, and so forth) matrix elements, which are calculated as

$$\begin{aligned} \Delta W_{jk} &= \sum_m \begin{cases} \Delta W_{jjm} \\ \Delta W_{jkm} + \Delta W_{kjm} \end{cases} \\ &= \sum_m \frac{1}{4hc}{P'_3}^2 \begin{cases} \Theta_{jkm} & j = k \\ \frac{1}{2}(\Theta_{jkm} + \Theta_{kjm}) & j \neq k \end{cases} \end{aligned} \tag{10}$$

The solution of the obtained 12th order secular equation gives the frequencies and intensities of the $(SF_6)_2$ dimer in inert low-temperature matrixes.

In the case of nitrogen, there is an additional contribution to the energy U due to an interaction of the N_2 quadrupole moment with each of 12 dipole moments of the $(SF_6)_2$ dimer. The interaction energy U_{jm} of the dipole moment P_j with the quadrupole moment Q_m is represented as[24]

$$U_{jm} = \frac{3Q_m P_j \Lambda_{jm}}{2R_{jm}^4} \tag{11}$$

where $\Lambda_{jm} = 5 \cos \theta_p \cos^2 \theta_q - 2 \cos \theta_{pq} \cos \theta_q - \cos \theta_p$, θ_p is an angle between the unit vectors $\vec{e}_j$ and $\vec{e}_{jm}$, θ_q is an angle between $\vec{o}_m$ and $\vec{e}_{jm}$, and θ_{pq} is an angle between $\vec{e}_j$ and $\vec{o}_m$, where the unit vector $\vec{o}_m$ specifies the orientation of the N_2 molecule, $\vec{R}_{jm}$ is the distance between the jth dipole and Q_m quadrupole moments ($Q_m = 1.1$ atomic units). The total energy of an interaction of all quadrupole moments Q_m with the jth dipole of the $(SF_6)_2$ dimer ($j = 1,..., 0.12$) is $U_j = \sum_m U_{jm}$, where m is the number of nitrogen molecules.

The matrix elements that describe the dimer absorption spectrum for dipole–quadrupole interactions of anharmonic C–F oscillators are calculated as[25]

$$\Delta\tilde{W}_{jk} = \left(\frac{\partial U_j}{\partial q_k}\right)_0 \cdot 3\xi \tag{12}$$

where $\xi = [(x)/(2\omega)]^{1/2} = 0.045$ is the parameter of the Morse oscillator and the nonzero diagonal matrix elements are

$$\Delta\tilde{W}_{jk} = \sum_m \frac{3Q_m\Lambda_{jm}}{2R_{jm}^4}\left(\frac{\partial P_j}{\partial q_k}\right)_0 \cdot 3\xi = \begin{cases} \sum_m \frac{3Q_m\Lambda_{jm}}{2R_{jm}^4}\frac{P'_3}{\sqrt{2}}3\xi & j = k \\ 0 & j \neq k \end{cases} \tag{13}$$

The solution of secular eq 6 with supplements $\Delta W_{jk} + \Delta\tilde{W}_{jk}$ to diagonal elements and supplements ΔW_{jk} to off-diagonal elements yields the frequencies and intensities of $(SF_6)_2$ dimer vibrations in nitrogen matrixes.

VII. Calculation of the Structure of Nitrogen Matrixes Doped with $(SF_6)_2$ Dimers

The structure of doped matrixes was calculated by the Monte Carlo method using the modification of the classic Metropolis algorithm and periodic boundary conditions.[26,27] The cubic box containing several hundred N_2 particles and a rigid $(SF_6)_2$ dimer was used in the calculation. The dimer was located at the center of the cell, and the axis of the dimer was directed along the z axis of the cell. The rigid dimer structure was the same as that in a molecular beam. It is described by the D_{2d} symmetry group and $R_{SS} = 4.754$ Å[13] (see Figure 4). After a number of displacements, the ensemble reached a stationary state in which its energy H was minimal and, on the average, the configuration of the system, consisting of the M host particles and the $(SF_6)_2$ dimer, did not change any more. Similar calculations in the Ar matrix were carried out earlier.[18]

We assume that each nitrogen atom of one of the N_2 molecules interacts with all of the remaining M atoms and all the dimer atoms (two S atoms and 12 F atoms). It is also assumed that the N_2 molecules are rigid and change their positions as a whole. The position of a N_2 molecule is determined by three Cartesian coordinates of the center of mass and two angles. In the course of the calculation, the position of the mth molecule of the matrix was randomly changed by a value not exceeding ε_1 ($x_{mi} \rightarrow x_{mi} + \alpha_{mi}\varepsilon_1$), where α_{mi} is a random number, such that $|\alpha_{mi}| < 1$, $i = 1, 2, 3$ and $m = 1, 2,..., N$), while the orientation of the mth molecule was randomly changed by a value not larger than ε_2 ($\varphi_{mi} \rightarrow \varphi_{mi} + \alpha_{mi}\varepsilon_2$), where α_{2i} is a random number, $|\alpha_{mi}| < 1$, $i = 4, 5$, and $m = 1, 2,..., N$. As an interaction potential, we used the set of Barker–Pompe atom–atom potentials, which are modifications of the Buckingham potential[28] that provides the realistic description of the attractive and repulsive forces

$$V(R_{mn}) = B_{mn} \cdot \exp[-\Omega_{mn} R_{mn}] - A_{mn} \cdot R_{mn}^{-6} \tag{14}$$

Here, R_{mn} is the distance between the centers of mass of the mth and nth atoms, $B_{mn} = B_m B_n$, $A_{mn} = A_m A_n$, and $\Omega_{mn} = \Omega_m + \Omega_n$. The following parameters of potentials were used in the calculations: B_m= 552.8, 471.9, 579.8, and 735.4 (kJ mol^{-1})$^{1/2}$; A_m = 81.50, 39.79, 24.55, and 88.24 (kJ mol^{-1} Å^6)$^{1/2}$; and Ω_m= 1.660, 1.755, 2.064, and 1.566 Å^{-1} for the Ar, N, F, and S atoms, respectively.[28]

The previous computer simulation for argon matrixes with a model cell containing from 512 to 1440 particles demonstrated[18] that the optimum number of particles M for these calculations is about 800. The calculations with a smaller number of particles are characterized by a large scatter of the results. An increase in the number of particles is inexpedient because it leads to a considerable increase in the computer time. Thus, the calculations for nitrogen were made with 864 molecules. The density of nitrogen at 10 K was estimated to be 0.040 mol/cm^3.[29] It was shown that a 5% change in this density has no effect on the calculated structure. It is supposed that the initial condition coincides with the initial condition for nitrogen α-N_2,[30] and the centers of nitrogen molecules were located at the center of a regular face-centered lattice.

As a result of calculations, we obtain a set of equilibrium structures, which differ from each other by the symmetry of the environment of the $(SF_6)_2$ dimer. It is clear that the positions of particles of the matrix located at the center of the regular lattice should be changed first of all to provide a necessary space for the dimer. This perturbation leads to a change in the positions of a considerable number of particles in the box.

As an example, Figure 6 shows the cross sections of the box by the XZ plane, with the $(SF_6)_2$ dimer axis lying in this plane. The thickness of the cross section is 0.2 Å, and the N atom diameter is 3.0 Å. Molecules of nitrogen are schematically shown as cylinders, and the distance between nitrogen atoms is $R_{NN} = 1.0975$ Å. The truncated cones mark N_2 molecules whose centers are outside of a plane. Note that the calculation for more than 19 systems, including the $(SF_6)_2$ dimer and 864 molecules of nitrogen, shows that the difference in energy of all configurations does not exceed 0.5%

For each configuration, the position and orientation of all molecules are known, and it is possible to calculate the amendment to matrix elements that describe the dimer absorption spectrum[4,10,18] by considering the DID (dipole–induced-dipole) interaction or DID plus dipole–quadrupole interaction. The solution of the secular eq 6 yields the frequencies and intensities of the 12 vibrational modes of the dimer. Nine of

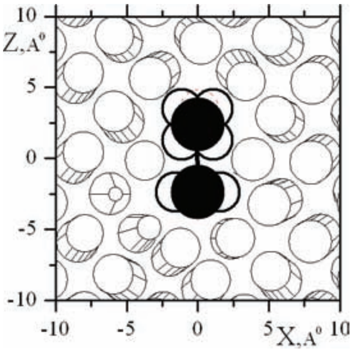

Figure 6. Cross section of a model cell in the *ZX* plane for a random configuration of molecules in a N_2 matrix. The thickness of the cross section is 0.2 Å, the diameter of the nitrogen atom is 3 Å, and M = 864.

these modes have practically zero intensity, while the intensities of three vibrations (denoted as $\nu_Z < \nu_Y \leq \nu_X$) are close to unity ($I > 0.98$). The spectral parameters of a dimer in a nitrogen matrix obtained by the computer simulation are presented in Table 3, which lists the results of the calculation of vibrational frequencies and splitting values for 19 systems with the DID interaction taken into account (columns I). Columns II of Table 3 show the spectral parameters calculated for the same 19 systems with an additional allowance made for the dipole−quadrupole interaction. It is seen from Table 3 that, on the whole, the spread in the values of ν_Z, ν_X, $\nu_D = (\nu_Z + \nu_X + \nu_Y)/3$ and $\Delta\nu = \nu_{X,Y} - \nu_Z$ calculated for 19 random configurations is small. The last row in Table 3 which is marked as "A" shows average values of spectral parameters. The frequencies of the dimer bands ν_Z, ν_Y, and ν_X and the splitting values $\Delta\nu$ calculated for the nitrogen matrix virtually do not differ from the corresponding parameters calculated for the argon matrix.[18]

The calculated frequencies ν_Z, ν_X, and ν_D and splitting values $\Delta\nu$ do not depend appreciably on the inclusion of the DID interaction or the DID plus dipole−quadrupole interaction. The greatest discrepancy was obtained for the value of splitting $|\delta| = \nu_X - \nu_Y$, which is equal to 0 for the $(SF_6)_2$ dimer in a molecular beam. The splitting parameter δ increases from 0.18 cm^{-1} for the model with the DID interaction to 1.2 cm^{-1} for the model with dipole−quadrupole interaction. The last value is in satisfactory agreement with the experimental splitting of $\delta = 0.9$ cm^{-1}. It is also seen from Table 3 that it is difficult to choose an optimal structure from the set of the simulated structures because the total energies $|H|$ of these systems virtually

TABLE 3: Frequencies ν_Z, ν_X, and $\nu_D = (\nu_Z + \nu_X + \nu_Y)/3$, Splitting Values $\Delta\nu$ and δ (CM^{-1}) of the $(SF_6)_2$ Dimer (f = 0.7 Å) in the Nitrogen Matrix, M = 864, and the Potential Energy $|H|$ (kJ/mol)

	ν_Z		ν_X		ν_D		$\Delta\nu$		δ		
	I	II	I	II	I	II	I	II	I	II	$\lvert H\rvert$
1	929.69	929.69	947.14	947.00	941.36	941.36	17.63	17.56	0.20	0.52	1823
2	929.59	929.67	947.13	947.16	941.31	941.48	17.58	17.71	0.07	0.51	1828
3	929.73	929.83	947.20	946.82	941.43	941.53	17.55	17.55	0.16	1.14	1830
4	929.40	928.64	947.20	947.68	941.32	941.33	17.88	19.24	0.17	0.41	1824
5	929.23	929.55	946.98	945.89	941.19	941.16	17.93	17.42	0.36	2.14	1825
6	929.52	928.56	947.07	947.76	941.31	941.58	17.63	19.53	0.22	0.66	1825
7	929.51	929.33	947.21	946.64	941.34	941.28	17.74	17.93	0.08	1.21	1825
8	929.62	929.41	947.21	946.95	941.40	941.40	17.67	17.97	0.15	0.44	1825
9	929.42	929.40	947.01	946.63	941.21	941.17	17.72	17.65	0.22	0.83	1819
10	929.47	929.39	947.00	946.74	941.25	941.19	17.67	17.71	0.31	0.71	1817
11	929.42	929.47	946.99	946.67	941.21	941.16	17.68	17.53	0.23	0.66	1821
12	929.67	929.19	947.07	947.22	941.26	941.57	17.59	18.62	0.11	1.03	1834
13	929.55	929.33	947.23	946.69	941.37	941.30	17.74	18.21	0.13	1.69	1826
14	929.67	929.71	947.23	947.00	941.40	941.38	17.60	17.50	0.05	0.40	1825
15	929.61	929.79	947.19	946.98	941.40	941.42	17.65	17.45	0.17	0.52	1831
16	929.59	928.72	947.04	946.54	941.34	941.36	17.61	19.06	0.31	2.51	1833
17	929.63	934.51	947.14	945.70	941.37	941.28	17.61	13.12	0.20	3.90	1827
18	929.57	930.01	947.14	945.14	941.35	941.18	17.67	16.71	0.20	3.15	1824
19	929.67	930.40	947.20	946.20	941.36	941.32	17.58	16.38	0.08	1.17	1817
A	929.6 ± 0.1	929.7 ± 0.6	947.1 ± 0.1	946.7 ± 0.5	941.3 ± 0.1	941.3 ± 0.1	17.7 ± 0.1	17.6 ± 0.8	0.18 ± 0.07	1.2 ± 0.7	

TABLE 4: Experimental and Calculated Frequencies ν_Z, ν_X, ν_Y, and ν_D and Splitting $\Delta\nu$ and δ (cm^{-1}) of $(SF_6)_2$ Dimer [Molecular Beam[13] (1), Averaged Spectral Parameters of $(SF_6)_2$ Dimers in Ar[15] (2) and in N_2 (3) Matrixes, Calculation in the Gas Phase (4), in an Ar Matrix with DID Interactions (5), in a N_2 Matrix with DID Interactions (6)[a] and (8)[b], and in a N_2 Matrix with DID + Dipole−Quadrupole Interactions (7)[a] and (9)[b]]

	system	ν_Z	ν_X	ν_Y	ν_D	$\Delta\nu$	δ
	Experimental Values						
1	molecular beam	934.007	956.078	956.078	948.734	22.07	0
2	Ar matrix	926.65(2)	945.10(2)	945.10(2)	937.1(4)	18.45(4)	0
3	N_2 matrix	929.1(1)	941.0(1)	941.9(1)	937.3(1)	12.4(2)	0.9(2)
	Calculated Values with Correction for the DID Interaction between SF_6 Molecules From Equation 8						
4	the gas phase	933.0	954.9	954.9	947.5	21.9	0
5	Ar matrix with DID interaction	927.8(2)	946.9(2)	947.0(2)	940.5(2)	19.1(2)	0.08(6)
6	N_2 matrix with DID interaction	927.9(1)	946.3(1)	946.5 (1)	940.4(1)	19.0(1)	0.18(7)
7	N_2 matrix with DID + D−Q interactions	928.0(6)	946.3(5)	947.5(5)	940.4(1)	18.9(8)	1.2(7)
8	N_2 matrix with DID interaction with R_{SS} = 5 Å	929.8(1)	945.8(2)	946.0(2)	940.5(1)	16.1(1)	0.25(13)
9	N_2 matrix with DID + D−Q interactions with R_{SS} = 5 Å	930(2)	945.4(6)	946.7(4)	940.5(2)	16(2)	1.4(9)

[a] R_{SS} = 4.747 Å. [b] R_{SS} = 5 Å; the figures in parentheses are the standard deviations.

coincide. For this reason the root-mean-square error of $\Delta\delta$ for 19 calculated structures equals 0.7 cm^{-1}.

Table 4 shows the experimental and calculated frequencies and splitting values of the absorption spectra of $(^{32}SF_6)_2$ dimers in the molecular beam and in the low-temperature argon and nitrogen matrixes. One can see from Table 4 that the center of gravity ν_D of the complex band in matrixes is red shifted by ~11 cm^{-1} (lines 2 and 3) from the experimental molecular beam value (line 1). It is possible to reasonably describe the spectra of the dimer in the gas phase and in matrixes using the above-stated model. The calculated red shifts of about 7 cm^{-1} (lines 5, 6, 7, 8, and 9) with respect to the ν_D in the gas phase (line 4) are smaller than the experimental values. Note that for all of the models, the calculated frequencies in matrixes do not change significantly with $\nu_D = (940.4-940.5)$ cm^{-1}. As one can see from Table 4, the observed splitting value $\Delta\nu = \nu_{X,Y} - \nu_Z$ decreases upon transition from the gas phase to an argon matrix from 22.1 to 18.5 cm^{-1} and further to 12.4 cm^{-1} in a N_2 matrix. The calculated values of $\Delta\nu$ are in satisfactory agreement with the experimental values for the gas phase (line 4) and Ar matrix (line 5). We emphasize that the resonance splitting $\Delta\nu$ calculated for nitrogen matrixes both with the help of a model with DID interactions ($\Delta\nu = 19.0$ cm^{-1}, line 6) and with the help of the model with DID + dipole−quadrupole interactions ($\Delta\nu = 18.9$ cm^{-1}, line 7) considerably differs from the experimental value ($\Delta\nu = 12.4$ cm^{-1}, line 3).

Note also that the calculated $\delta = |\nu_Y - \nu_X|$ value is 0 only in the gas phase; for an argon matrix, our calculation gives the averaged value of $\delta = 0.08$ cm^{-1}. For a nitrogen matrix, the value of δ calculated with allowance for the DID interaction is considerably smaller than the experimental result, $\delta_{calc} < \delta_{exp} = 0.9$ cm^{-1}, while the inclusion of the DID + dipole−quadrupole interaction leads to $\delta_{calc} > \delta_{exp}$. For comparison, we have also calculated the spectral characteristics of the $(SF_6)_2$ dimer in the nitrogen matrix (for six independent systems) assuming that the R_{ss} distance is increased from 4.747 up to 5 Å (lines 8 and 9). As one can see from Table 4, the value of resonance splitting $\Delta\nu$ decreases and approaches the experimental value, and the values of ν_D and δ do not change within the calculation error limit.

VIII. Conclusions

We have studied the absorption spectrum of $(^{32}SF_6)_2$, $(^{33}SF_6)_2$, and $(^{34}SF6)_2$ dimers in nitrogen matrixes at 11 K. The concentration dependences of the relative intensity of all bands were studied after deposition and after annealing at 30 K. The characteristics of the dimer bands are governed by the resonance dipole−dipole interaction between two SF_6 subunits. The absorption bands associated with the two types of dimers have been identified. It was shown that the doublet $\nu_{X,Y} = 949.0$ and $\nu_Z = 926.8$ cm^{-1} can be assigned to the dimer whose parameters are similar to parameters of the $(^{32}SF_6)_2$ dimer in the gas phase, where the triply degenerate ν_3 band is split into two $\nu_{X,Y}$ and ν_Z components. This dimer exists only after deposition and disappears after matrix annealing.

The spectrum of the stable $(SF_6)_2$ dimer in the nitrogen matrix is different from the dimer spectra in the argon matrix and in the gas phase. In solid nitrogen, the $(^{32}SF_6)_2$ dimer is characterized by a triplet with $\nu_X = 941.1$, $\nu_Y = 942.0$, and $\nu_Z = 929.2$ cm^{-1}. The *X* and *Y* components of resonance doublet are split in this matrix with $\delta = |\nu_Y - \nu_X| = 0.9$ cm^{-1}. The value of the resonance splitting $\Delta\nu = (\nu_X + \nu_Y)/2 - \nu_Z$ is equal to ~12.4 cm^{-1} and is appreciably smaller than a value of $\Delta\nu = 18.45$ cm^{-1} in an argon matrix.

By using the computer simulation method, we attempted to determine the matrix effect on the dimer spectra. The model developed involves (a) the calculation of the resonance spectrum of an isolated dimer in terms of the local-mode model, (b) the Monte Carlo simulation of the N_2 matrix structure containing the rigid $(SF_6)_2$ dimer and 864 N_2 molecules, and (c) the calculation of the dimer spectra taking into account the dipole−induced-dipole interactions between all point dipoles located on each of the S−F bonds of $(SF_6)_2$ dimer and N_2 particles and also the interaction between the quadrupole moment of N_2 molecules and dipole moments of $(SF_6)_2$ dimers.

The solution of the secular equation for $(SF_6)_2$ gives the frequencies and intensities of 12 stretching vibrations of the $(SF_6)_2$ dimer in N_2 matrixes. The calculated spectra sufficiently well reproduce the main characteristics of the experimental spectra, in particular, the decrease of the resonance splitting upon transition from the gas phase to the N_2 matrix and the splitting of $\nu_{X,Y}$ component in this matrix.

Acknowledgment. This study was supported by the Russian Foundation for Basic Research, Grants 06-03-32073 and 09-03-32272.

References and Notes

(1) Gough, T. E.; Knight, D. G.; Scoles, G. *Chem. Phys. Lett.* **1983**, *97*, 155.
(2) Gough, T. E.; Knight, D. G.; Rowntree, P. A.; Scoles, G. *J. Phys. Chem.* **1986**, *90*, 4026.
(3) Snels, M.; Reuss, J. *Chem. Phys. Lett.* **1987**, *140*, 543.
(4) van Bladel, J. W. I.; van der Avoid, A. *J. Chem. Phys.* **1990**, *92*, 2837.
(5) Levander, D. J.; Goyal, S.; McComble, J.; Pate, B.; Scoles, G. *J. Chem. Soc., Faraday. Trans.* **1990**, *86*, 2361.
(6) Urban, R.-D.; Takami, M. *J. Chem. Phys.* **1995**, *102*, 3017.
(7) Kolomiitsova, T. D.; Burtsev, A. P.; Fedoseev, V. G.; Shchepkin, D. N. *Chem. Phys.* **1998**, *238*, 315.
(8) Knozinger, E.; Babka, E.; Hallamasek, D. *J. Phys. Chem. A* **2001**, *105*, 8176.
(9) Katsuki, H.; Momose, T.; Shida, T. *J. Chem. Phys.* **2002**, *116*, 8411.
(10) Cherevatova, A. V.; Kolomiitsova, T. D.; Shchepkin, D. N.; Tokhadze, K. G.; Mielke, Z.; Coussan, S.; Roubin, P. *J. Mol. Spectrosc.* **2006**, *238*, 65.
(11) Gough, T. E.; Mengel, M.; Rowntree, P. A.; Scoles, G. *J. Chem. Phys.* **1985**, *83*, 4958.
(12) Gu, X. J.; Levander, D. J.; Zhang, B.; Scoles, G.; Zhuang, D. *J. Chem. Phys.* **1990**, *93*, 4898.
(13) Urban, R.-D.; Takami, M. *J. Chem. Phys.* **1995**, *103*, 9132.
(14) Beu, T. A.; Takeuchi, K. *J. Chem. Phys.* **1995**, *103*, 6394.
(15) Kolomiitsova, T. D.; Mielke, Z.; Shchepkin, D. N.; Tokhadze, K. G. *Chem. Phys. Lett.* **2002**, *357*, 181.
(16) Ignatov, S. K.; Kolomiitsova, T. D.; Mielke, Z.; Razuvaev, A. G.; Shchepkin, D. N.; Tokhadze, K. G. *Chem. Phys.* **2006**, *324*, 753.
(17) Fox, K.; Person, W. *J. Chem. Phys.* **1976**, *64*, 5218.
(18) Tokhadze, I. K.; Kolomiitsova, T. D.; Tokhadze, K. G.; Shchepkin, D. N. *Opt. Spectrosc.* **2007**, *102*, 396.
(19) Kolomiitsova, T. D.; Burtsev, A. P.; Peganov, O. G.; Shchepkin, D. N. *Opt. Spectrosc.* **1998**, *84*, 381.
(20) Mielke, Z.; Tokhadze, K. G.; Latajka, Z.; Ratajczak, E. *J. Phys. Chem.* **1996**, *100*, 539.
(21) Kolomiitsova, T. D.; Melikova, S. M.; Miroshnichenko, G. P. *Opt. Spectrosc.* **1985**, *59*, 735.
(22) St.-Arnaud, J. M.; Bose, T. K. *J. Chem. Phys.* **1979**, *71*, 4951.
(23) Sage, M. L.; Williams, J. A., III. *J. Chem. Phys.* **1983**, *78*, 1348.
(24) Kielich, S. *Molekularna optyka nieliniowa*; PWN: Warszawa-Poznan, 1977.
(25) Buckingham, A. D. *Trans. Faraday Soc.* **1960**, *56*, 753.
(26) Metropolis, N. A.; Rosenbluth, A. W.; Rosenbluth, M. N.; Teller, A. H.; Teller, E. *J. Chem. Phys.* **1953**, *21*, 1087.
(27) Allen, M. P.; Tildesley, D. J. *Computer Simulation of Liquids*; Clarendon Press: Oxford, U.K., 1991; p 110.
(28) Kaplan, I. G. *Theory of Molecular Interactions*; Nauka: Moscow, 1982, (Engl. Transl.) Elsevier: New York, 1986.
(29) Malkov, M. P. *Physicotechnical Fundamentals of Cryogenics*; Énergiya: Moscow, 1973 [in Russian].
(30) Kobashi, K.; Etters, R. D. *J. Chem. Phys.* **1985**, *82*, 4341.

JP902055M